



# Projecting climate change impacts on rainfed wheat yield, water demand, and water use efficiency in northeast Iran

Parisa Paymard<sup>1</sup> · Fatemeh Yaghoobi<sup>2</sup> · Milad Nouri<sup>3,4</sup> · Mohammad Bannayan<sup>2</sup>

Received: 9 June 2017 / Accepted: 6 May 2019 / Published online: 28 May 2019  
© Springer-Verlag GmbH Austria, part of Springer Nature 2019

## Abstract

The frequency and severity of high temperature and drought extremes are expected to increase under future climate change (CC) and considerably affect the agricultural sector particularly in water-limited ecosystems. This study was conducted to assess future CC impacts on rainfed wheat yield, water requirement (CWR), water use efficiency (WUE), precipitation use efficiency (PUE), reference crop evapotranspiration ( $ET_0$ ), and agricultural rainfall index (ARI) in northeast of Iran. The outputs of five global climate models (GCMs) under RCP-4.5 and RCP-8.5 during three time periods (i.e., the 2025s, 2055s, and 2085s) downscaled by MarkSimGCM model were applied. CWR was estimated using the CROPWAT 8.0 model. Further, the CSM-CERES-Wheat model was employed to simulate rainfed wheat yield, WUE, PUE, and  $ET_0$  responses to CC. The results showed that the mean monthly  $ET_0$  and CWR would likely increase under both emission pathways over the studied sites. The mean monthly ARI is also anticipated to decline in the future indicating a drier climatic condition over northeastern Iran by 2100. Furthermore, CC is highly likely to decrease rainfed grain yield, WUE, and PUE during the current century. The largest changes in  $ET_0$ , ARI, CWR, yield, WUE, and PUE were projected in the late twenty-first century (the 2085s) under RCP-8.5. The CC-induced wheat yield loss will likely endanger food security in the country. Yield reduction can be partially offset by adopting appropriate adaptation measures.

## 1 Introduction

Water scarcity is the most limiting factor negatively affecting agricultural production in water-limited environments (Rockström et al. 2010). Climate change (CC) as a result of enhanced greenhouse gas concentrations seems to aggravate water stress in such areas (IPCC 2013). Large-scale climate anomaly events such as the El Niño–Southern Oscillation (ENSO) were projected to be stronger and more frequent owing to CC (Cai et al. 2014, 2015). Therefore, ENSO-driven weather

extremes such as drought and high temperatures are anticipated to be more recurrent and severe across the globe. The Middle East and North Africa (MENA) is a drought-prone region highly affected by persistent drought spells (Sowers et al. 2011). Due to reduced storm track activity, droughts are likely to be more frequent and intensive for the rest of the twenty-first century (Evans 2009). Thus, already drought-affected regions such as Iran will experience more dry episodes in the future (Li et al. 2009; Araghi et al. 2018). Considering the growing population (at least until 2050), more agricultural outputs are, however, needed to be produced under climatically undesirable conditions for more people (Rockström et al. 2009).

Iran is located within an arid and semi-arid belt and relatively scant annual precipitation mainly falls from October through April (Bannayan et al. 2010; Araghi et al. 2015, 2018; Nouri and Homaei 2018). Dry farming in west, north-west, and northeast Iran is possible owing to above-normal precipitation and fertile plains in these semi-arid regions (Bannayan et al. 2011; Nouri et al. 2017a; Paymard et al. 2018). Wheat (*Triticum aestivum* L.) as the staple food in Iran is mostly cultivated under rainfed conditions (Iran Ministry of Agriculture 2015). However, wheat yield and water productivity in Iran are low due to mismanagement and precipitation anomalies (Nouri et al. 2017a; Faramarzi et al. 2010). In

✉ Parisa Paymard  
paris.p664@yahoo.com

<sup>1</sup> Department of Agriculture, Islamic Azad University - Mashhad Branch, P.O. Box 91735–413, Mashhad, Iran

<sup>2</sup> Faculty of Agriculture, Ferdowsi University of Mashhad, P.O. Box 91775–1163, Mashhad, Iran

<sup>3</sup> Faculty of Agriculture, Tarbiat Modares University, P.O. Box 14115–336, Tehran, Iran

<sup>4</sup> National Agriculture and Water Strategic Research Center, Iran Chamber of Commerce, Industries, Mines and Agriculture, Tehran, Iran

addition, rainfed wheat yield fluctuates greatly over semi-arid regions causing some adverse socioeconomic impacts (Bannayan et al. 2010, 2011). Bannayan et al. (2011) attributed 30–50% of rainfed cereal yield variation to precipitation anomalies in northeast Iran. In addition, correlation coefficient between rainfed wheat yield and rainfall amount ranged between 0.3 and 0.72 in west and northwest Iran (Nouri et al. 2017a). Thus, drought adversely influences rainfed wheat yield, and drought-caused yield reduction is expected to be larger in the future. Nouri et al. (2016) reported rainfed wheat yield decrease over 2071–2099 in the western drylands of Iran particularly for the heavier-textured soils under Intergovernmental Panel on Climate Change (IPCC) fifth assessment report (AR5) representative concentration pathways (RCPs). A considerable change in rainfed wheat production ranging from –28 to 56% during the twenty-first century with respect to the baseline (1961–1990) period was projected by Bannayan and Eyshi Rezaei (2014) for northeastern Iran under IPCC AR4 (fourth assessment report) scenarios.

Crop water requirement (CWR) is defined as the water amount required to meet evapotranspiration loss of a disease-free crop, growing in a large field under no soil water stress and achieving potential production in a given growing season (Jensen and Allen 2016). Calculation of CWR helps planners in scheduling and allocating irrigation (Todorovic 2005). CWR can be estimated by multiplying the crop coefficient ( $K_c$ ) and reference crop evapotranspiration ( $ET_0$ ) (Allen et al. 1998; Jensen and Allen 2016). Therefore, CC greatly influences CWR through changing  $ET_0$  (Tabari et al. 2011; Nouri et al. 2017b, c). The CC-induced increment in CWR seems to have more severe consequences for the agriculture sector in water-limited environments due chiefly to already depleted water resources and projected rainfall shortage in these fragile ecosystems. Furthermore, a 3.0 °C increase in atmospheric temperature is likely to be experienced in drylands if the Paris Agreement aims to limit warming to 1.5 °C relative to pre-industrial levels will be met (Huang et al. 2017). Therefore, CC appears to have more adverse impacts on  $ET_0$  and CWR in water-limited regions such as Iran. There are some studies focused on CWR response to CC under irrigation (blue water) (Yang et al. 2013; Ashofteh et al. 2015). However, CWR which is fulfilled by soil water (green water storage) has not yet been well addressed in changing climates over rainfed croplands vis-à-vis irrigated plains (Luo et al. 2015).

In dryland farming systems, maximizing produced crop per drop of rain is the major objective (Stewart and Steiner 1990; Rockström et al. 2002). Putting it differently, enhancing the ratio of yield per unit of water lost via evapotranspiration or water use efficiency (WUE) is of high significance for rainfed agriculture in water-limited areas. Improving rainfed yield by manipulating vapor shift in favor of transpiration is a robust adaptation option for dryland farming (Rockström et al. 2010; Nouri et al. 2017d). WUE is expected to be greatly affected by CC through the

twenty-first century. Guo et al. (2010) projected 9.2–74.9% increase in wheat WUE in the North China Plain during the current century. An increment in wheat WUE ranging from 7 to 10% under different scenarios in the twenty-first century was simulated by Mo et al. (2009) over the North China Plain. Wang et al. (2011) concluded that wheat WUE would likely increase by 7–33% in wetter regions and decrease by 6–14% in drier areas of southeast Australia in the future. Yang et al. (2016) also reported that WUE of rainfed wheat over semi-arid environments of southeastern Australia will increase by 0.7–1.3 ( $\text{kg ha}^{-1} \text{mm}^{-1}$ ) in 2021–2040. WUE rise was majorly ascribed to higher efficiency of crop growth under  $\text{CO}_2$  fertilization. However, increase of WUE and yield seems unlikely under drier scenarios in water-limited regions. Another useful indicator for assessing the yield production efficiency under rainfed condition is precipitating use efficiency (PUE) defined as yield produced per unit of precipitation received (Peterson and Westfall 2004; Wang et al. 2016). This study was aimed to assess the impact of CC on rainfed wheat yield, CWR, WUE, PUE,  $ET_0$ , and drought trend over the period of 2011–2040 (2025s), 2041–2070 (2055s), and 2071–2099 (2085s) with respect to the baseline period (1961–1990) in northeastern Iran.

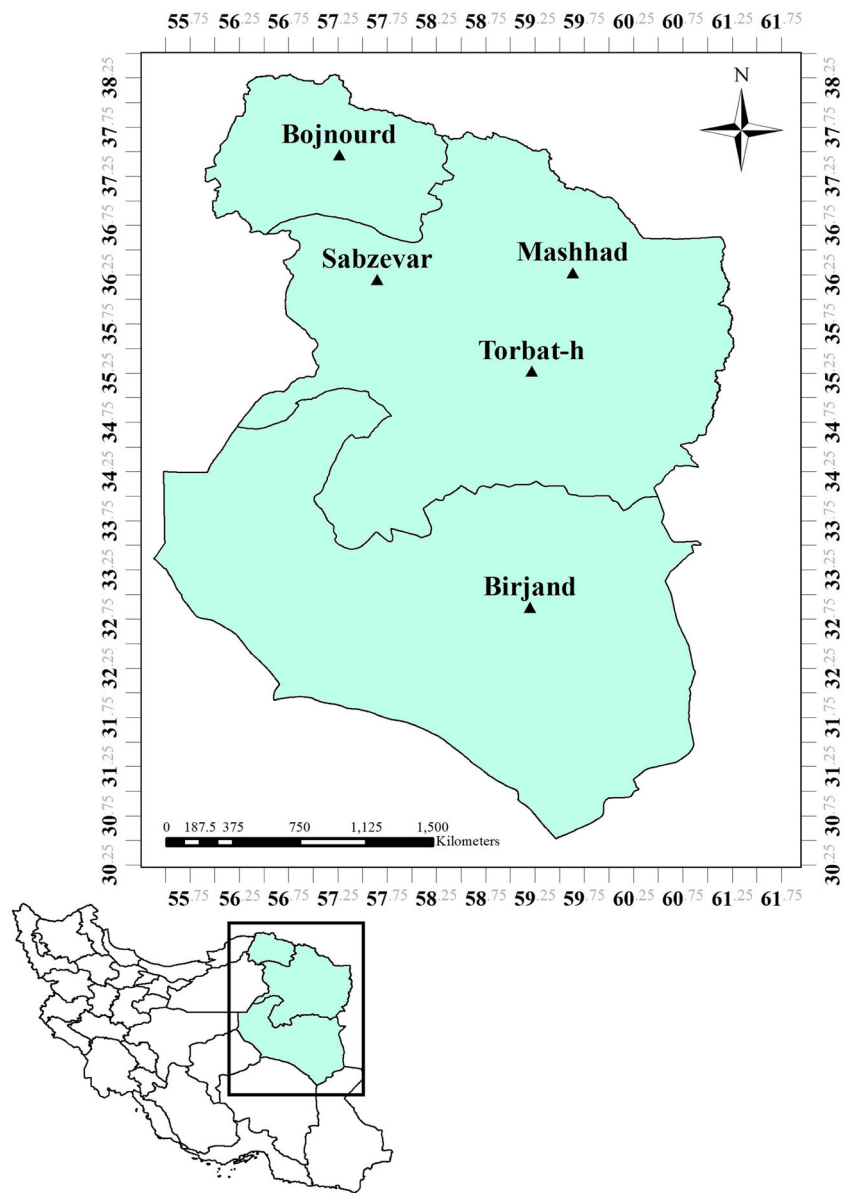
## 2 Materials and methods

### 2.1 Study area and climatic data

This study focused on Khorasan Province located in northeast Iran. Five locations including Birjand, Bojnourd, Mashhad, Sabzevar, and Torbat-h lying between 32° and 37° N latitudes and 57° and 59° E longitudes were investigated (Fig. 1 and Table 1). In general, these locations have arid (Birjand and Sabzevar) and semi-arid (Bojnourd, Mashhad, and Torbat-h) climates. Moreover, Bojnourd is the wettest site and Birjand is the most arid station among these sites (Table 1).

MarkSimGCM model downscaling the large-scale global circulation model (GCM) outputs to a  $0.5^\circ \times 0.5^\circ$  latitude/longitude grid resolution was used. The model downscales the GCM data based on climate typing techniques and stochastic downscaling (Jones and Thornton 2013, 2015). Precipitation series are synthesized by applying third-Markov stochastic model. Furthermore, the generation of daily minimum and maximum temperatures and solar radiation data occurs on the basis of the approach proposed by Richardson (1981). The baseline period data (1961–1990) in MarkSimGCM are gathered from the WorldClim database (Jones and Thornton 2013). The WorldClim (<http://www.worldclim.org>) provides the representative baseline (current) climate conditions (i.e., 1961–1990) (Jones and Thornton 2013). It uses historical data retrieved from some datasets covering a large number of stations over the globe. It also applies the thin plate smoothing method with a fixed lapse rate by the ANUSPLIN program.

**Fig. 1** The location of investigated sites



Further details on the algorithm are described by Hutchinson (1997). The simulation outputs of five CMIP5 (fifth phase of Coupled Model Intercomparison Project) GCMs, i.e., BCC-CSM 1.1(m), FIO-ESM, GFDL-ESM2M, IPSL-CM5A-LR,

and MIROC-ESM-CHEM for RCP-4.5 and RCP-8.5, were an ensemble to provide the future climatic conditions. The details of these five GCMs are presented in Table 2. RCP-4.5 is a midrange climate change scenario assuming that some land- and energy-related mitigations would be undertaken to make the radiative forcing stable at  $4.5 \text{ W m}^{-2}$  by 2100 (Thomson et al. 2011). RCP-8.5 which stands for a radiative forcing of  $8.5 \text{ W m}^{-2}$  by the end of the current century, however, conveys a business-as-usual condition without any mitigation policy (Riahi et al. 2011). For each time period (future and past), 30 years of daily climate data (as the replicates) were projected. Furthermore, the performance of MarkSimGCM was statistically evaluated by comparing recorded and model-generated data over the baseline period (1961–1990). The recorded daily maximum ( $T_{\max}$ ) and minimum ( $T_{\min}$ ) temperatures ( $^{\circ}\text{C}$ ),

**Table 1** Geographic characteristics, climate classification, and soil texture of the studied sites over the 1961–1990

Location	LAT (dd)	LON (dd)	Altitude (m)	Climate	Soil texture
Bojnourd	37.28	57.19	1091	Semi-arid	Loam
Birjand	32.52	59.12	1491	Arid	Loam
Mashhad	36.16	59.38	999	Semi-arid	Clay loam
Torbat-h	35.16	59.13	1450	Semi-arid	Sandy loam
Sabzevar	36.12	57.43	977	Arid	Loam

**Table 2** The used global climate models and their grid resolution

Model name	Model acronym	Grid resolution		Reference
		Latitude	Longitude	
Beijing Climate Center	BCC-CSM 1.1(m)	2.81°	2.81°	Wu (2012)
First Institute of Oceanography-Earth System Model	FIO-ESM	2.81°	2.81°	Song et al. (2012)
Geophysical Fluid Dynamics Laboratory Earth System Model with MOM, version 4 component	GFDL-ESM2M	2.00°	2.50°	Dunne et al. (2012)
Institute Pierre-Simon Laplace Coupled Model, version 5A, low resolution	IPSL-CM5A-LR	1.87°	3.75°	Dufresne et al. (2013)
Model for Interdisciplinary Research on Climate, Earth System Model, Chemistry Coupled	MIROC-ESM-CHEM	2.81°	2.81°	Watanabe et al. (2011)

rainfall ( $\text{mm day}^{-1}$ ), and solar radiation ( $\text{MJ m}^{-2}\text{day}^{-1}$ ) were obtained from Iran Meteorological Organization (IRIMO) for the period 1961–1990.

## 2.2 Agricultural rainfall index

Agricultural rainfall index (ARI) was employed to investigate the drought severity and persistence over the studied areas. ARI represents a reliable indicator for monthly water balance and is employed to quantify agricultural droughts (Ghazalli and Nieuwolt 1982; Nieuwolt 1989; Sayari et al. 2013). ARI is computed as follows:

$$\text{ARI} = \left( \frac{P}{\text{ET}_0} \right) \times 100 \quad (1)$$

where  $P$  is monthly precipitation.

The values of  $< 40$  for ARI indicate drought occurrence in a given month. When  $40 < \text{ARI} < 200$ , the condition is favorable for vegetation and agricultural production. ARI above 200 demonstrates a wet month (Nieuwolt 1989; Sayari et al. 2013).

## 2.3 Modeling

The rainfed wheat yield,  $\text{ET}_0$ , WUE, and PUE changes were projected using the Cropping System Model-Crop Environment Resource Synthesis-Wheat (CSM-CERES-Wheat). The CSM-CERES-Wheat is a computerized model included in the Decision Support System for Agrotechnology Transfer (DSSAT v4.7) software package widely employed to simulate wheat yield and phenology (Jones et al. 2003; Hoogenboom et al. 2017). The inputs required to parametrize the model include plant genetic coefficients, field and management details, soil physical and chemical properties, and climatic variables (Bannayan et al. 2016; Paymard et al. 2018).

The genetic coefficients of Sardari cultivar (a winter bread wheat cultivar commonly grown under rainfed condition in northeast Iran) already calibrated and validated by Eyshi Rezaie and Bannayan (2012) and Bannayan et al. (2014) were

used to run the CSM-CERES-Wheat. In general, the CSM-CERES-Wheat showed good performance in simulation wheat growth stages in northeast Iran (Eyshi Rezaie and Bannayan 2012; Bannayan et al. 2014). Moreover, the management-related parameters such as planting method, planting depth, planting distribution, fertilizer applications, row spacing, and plant population at seeding were those considered by Eyshi Rezaie and Bannayan (2012) and Bannayan et al. (2014).

There are two alternatives, i.e., the Penman–Monteith FAO-56 (PMF-56) equation (Allen et al. 1998) and the Priestley–Taylor (PT) model (Priestley and Taylor 1972), available in the CSM-CERES-Wheat to calculate  $\text{ET}_0$ . Since MarkSimGCM does not provide wind speed data needed to compute  $\text{ET}_0$  based on PMF-56 equation, the PT model was applied for  $\text{ET}_0$  estimation. PT is a simplified and shortened form of Penman's (1948)  $\text{ET}_0$  model considering a lumped coefficient to account for the aerodynamic features of  $\text{ET}_0$  (Pereira 2004). The mathematical expression of PT equation is:

$$\text{ET}_0 = \alpha \left( \frac{\Delta}{\Delta + \gamma} \right) \left( \frac{R_n - G}{\lambda} \right) \quad (2)$$

where  $\alpha$  is the model coefficient mostly considered to be 1.26,  $\text{ET}_0$  is the reference evapotranspiration ( $\text{mm day}^{-1}$ ),  $\Delta$  represents the slope of the saturation vapor pressure–temperature relationship ( $\text{kPa } ^\circ\text{C}^{-1}$ ) at the mean temperature point,  $\gamma$  is the local psychrometric constant ( $\text{kPa } ^\circ\text{C}^{-1}$ ),  $R_n$  denotes the net radiation ( $\text{MJ m}^{-2} \text{day}^{-1}$ ),  $G$  is the soil heat flux ( $\text{MJ m}^{-2} \text{day}^{-1}$ ), and  $\lambda$  is the latent heat of vaporization ( $\text{MJ kg}^{-1}$ ).

WUE and PUE are calculated by:

$$\text{WUE} = \frac{Y}{\text{ETc}} \quad (3)$$

$$\text{PUE} = \frac{Y}{P} \quad (4)$$

where  $Y$  is crop yield ( $\text{kg ha}^{-1}$ ),  $\text{ETc}$  is crop evapotranspiration (mm), and  $P$  is precipitation (mm) during the growing season.

CWR or actual crop evapotranspiration ( $\text{ETc}$ ) under standard condition was computed using CROPWAT 8.0. The software is

**Table 3** Comparison of modeled (*Mod.*) with recorded (*Rec.*) seasonal and annual average  $T_{max}$  data over 1961–1990

Location	Variable	Winter <sup>a</sup>		Spring <sup>b</sup>		Summer <sup>c</sup>		Autumn <sup>d</sup>		Annual	
		Rec.	Mod.	Rec.	Mod.	Rec.	Mod.	Rec.	Mod.	Rec.	Mod.
Bojnourd	Mean	7.22	7.04	18.93	19.58	31.57	31.74	21.38	20.84	19.83	19.85
	Variance	3.99	1.15	2.35	1.36	0.90	0.61	1.89	1.30	0.56	0.42
Birjand	Mean	12.48	13.18	24.68	24.66	34.99	35.07	25.92	25.98	24.57	24.75
	Variance	3.78	1.10	1.78	1.01	1.10	0.43	0.85	0.88	0.79	0.25
Mashhad	Mean	8.30	8.18	20.58	20.36	33.22	32.31*	22.24	21.72	21.14	20.64*
	Variance	7.42	1.15	1.63	1.34	0.75	0.59	1.69	1.01	0.86	0.33
Torbat-h	Mean	8.45	9.22	21.40	20.67	33.18	33.08	23.29	22.73	21.63	21.43
	Variance	5.03	1.18	2.27	1.31	1.38	0.53	1.39	0.96	1.03	0.30
Sabzevar	Mean	10.15	10.44	23.90	22.98	36.26	35.72*	25.39	24.79	23.98	23.49
	Variance	6.28	1.19	1.50	1.25	1.02	0.50	1.52	0.99	0.72	0.31

<sup>a</sup> December–January–February

<sup>b</sup> March–April–May

<sup>c</sup> June–July–August

<sup>d</sup> September–October–November

\*Significant difference at the level of 95%

designed to estimate CWR and irrigation demand for a wide range of climates and crops (FAO 2009; Luo et al. 2015). Furthermore, the program allows the development of irrigation schedules for different management conditions and the calculation of a water supply scheme for varying crop patterns (FAO 2009). The calculations considered in CROPWAT 8.0 are based on the procedures proposed by Allen et al. (1998) and Doorenbos and Kassam (1979). The CROPWAT 8.0 computes CWR or ETc using a two-step model introduced by Allen et al. (1998):

$$ET_c = K_c \times ET_0 \tag{5}$$

where  $K_c$  is the crop coefficient at different growth stages.

In this study,  $ET_0$  series already computed by the PT method was used as input data for the CROPWAT 8.0 software. In addition to  $ET_0$  and climatic data, the model requires some crop (e.g., sowing and harvesting dates, the length and  $K_c$  of different growing phases, rooting depth, and yield response fraction) and soil data. Wheat planting and harvesting data

**Table 4** Comparison of modeled (*Mod.*) with recorded (*Rec.*) seasonal and annual average  $T_{min}$  data over 1961–1990

Location	Variable	Winter <sup>a</sup>		Spring <sup>b</sup>		Summer <sup>c</sup>		Autumn <sup>d</sup>		Annual	
		Rec.	Mod.	Rec.	Mod.	Rec.	Mod.	Rec.	Mod.	Rec.	Mod.
Bojnourd	Mean	-2.88	-3.75	6.22	6.50	16.49	16.90	6.95	6.24	6.74	6.52
	Variance	1.84	1.36	0.37	1.97	1.09	0.60	0.33	2.50	0.17	0.39
Birjand	Mean	-1.27	-0.95	9.27	9.75	18.17	18.22	7.17	7.32	8.38	8.59
	Variance	1.70	0.98	1.36	1.15	1.38	0.54	1.71	1.41	0.91	0.28
Mashhad	Mean	-3.59	-3.01	7.34	6.94	16.26	15.86	5.72	5.77	6.47	6.43
	Variance	5.44	1.08	0.81	1.34	2.05	0.71	1.83	1.55	1.30	0.33
Torbat-h	Mean	-3.24	-3.07	7.53	7.25	17.68	16.98	6.47	5.93	7.16	6.83*
	Variance	3.55	1.08	0.74	1.36	0.67	0.68	1.02	1.55	0.48	0.33
Sabzevar	Mean	-1.14	-1.87	9.90	9.02	20.97	19.85*	9.49	9.20	9.86	9.09*
	Variance	3.36	1.00	1.19	1.21	2.65	0.54	2.55	1.36	1.24	0.29

<sup>a</sup> December–January–February

<sup>b</sup> March–April–May

<sup>c</sup> June–July–August

<sup>d</sup> September–October–November

\*Significant difference at the level of 95%



**Table 5** Comparison of modeled (*Mod.*) with recorded (*Rec.*) seasonal and annual average precipitation data over 1961–1990

Location	Variable	Winter <sup>a</sup>		Spring <sup>b</sup>		Summer <sup>c</sup>		Autumn <sup>d</sup>		Annual	
		Rec.	Mod.	Rec.	Mod.	Rec.	Mod.	Rec.	Mod.	Rec.	Mod.
Bojnourd	Mean	92.21	71.27	106.92	148.98	25.84	23.59	45.07	40.56	270.04	284.40
	Variance	1288.47	2363.04	2745.46	4209.83	839.67	503.76	611.71	682.27	6779.60	7610.87
Birjand	Mean	83.37	80.03	73.68	72.70	0.61	0.75	11.02	15.31	168.69	168.79
	Variance	1348.10	2821.69	1108.73	1363.77	1.75	1.90	122.17	188.08	2829.49	6924.06
Mashhad	Mean	96.34	94.89	126.32	153.06	4.59	13.56*	28.49	43.60	255.73	305.11
	Variance	1916.88	2590.80	2936.99	6506.15	32.29	404.04	555.18	1939.24	5132.10	16,952.52
Torbat-h	Mean	137.63	108.46	101.04	129.20	2.96	7.55	16.86	22.50	258.49	267.71
	Variance	3471.26	2943.37	1643.14	1752.39	22.15	186.10	258.10	829.04	5902.79	12,459.84
Sabzevar	Mean	89.81	83.13	76.65	85.97	3.70	12.42*	18.61	29.85	188.77	198.94
	Variance	1499.60	2522.11	1566.08	1403.28	57.02	278.62	304.06	1220.71	3703.29	6066.01

<sup>a</sup> December–January–February

<sup>b</sup> March–April–May

<sup>c</sup> June–July–August

<sup>d</sup> September–October–November

\*Significant difference at the level of 95%

were collected from local farmers and agriculture organization of the surveyed locations. The planting and harvesting dates, respectively, for wheat were considered to be 12 October and 14 May for Bojnourd, 17 November and 3 June for Birjand, and also 30 October and 23 May for Mashhad, Sabzevar, and Torbat-h. Moreover, the length and Kc for each wheat growing stage were obtained from Doorenbos and Kassam (1979) and Allen et al. (1998).

The standard Kc values of initial ( $K_{c_{ini}}$ ), mid- ( $K_{c_{mid}}$ ), and late ( $K_{c_{end}}$ ) growing season stages were set to be 0.40, 1.15, and 0.25 for winter wheat, respectively (Allen et al. 1998).  $K_{c_{mid}}$  and  $K_{c_{end}}$  (if the value of  $K_{c_{end}}$  is more than 0.45 in FAO tables) should be corrected according to local climate information. Therefore,  $K_{c_{mid}}$  value was corrected using the following:

$$K_{c_{mid}} = K_{c_{mid}(\text{Tab})} + [0.04(u_2 - 2) - 0.004(\text{RH}_{\min} - 45)](h/3)^{0.3} \quad (6)$$

where  $K_{c_{mid}(\text{Tab})}$  is the  $K_{c_{mid}}$  taken from FAO tables (Allen et al. 1998),  $u_2$  is the mean value for daily wind speed at 2 m

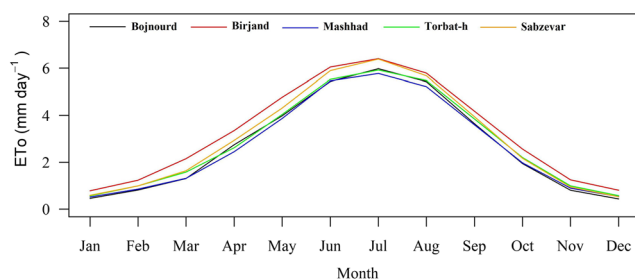


**Fig. 2** The monthly  $ET_0$  series for the baseline period (1961–1990)

height over grass during the mid-season growth stage ( $\text{m s}^{-1}$ ),  $\text{RH}_{\min}$  denotes mean value for daily minimum relative humidity during the mid-season growth stage (%), and  $h$  represents mean plant height during the mid-season stage (m).

The value of  $\text{RH}_{\min}$  for the sites was also computed as follows:

$$\text{RH}_{\min} = \frac{e^0(T_{\min})}{e^0(T_{\max})} \times 100 \quad (7)$$

$$e^0(T_{\min}) = 0.6108 \exp \left[ \frac{17.27 T_{\min}}{T_{\min} + 237.3} \right] \quad (8)$$

$$e^0(T_{\max}) = 0.6108 \exp \left[ \frac{17.27 T_{\max}}{T_{\max} + 237.3} \right] \quad (9)$$

where  $e^0(T_{\min})$  and  $e^0(T_{\max})$  are saturation vapor pressure at minimum and maximum daily air temperatures (kPa), respectively.

## 3 Results and discussions

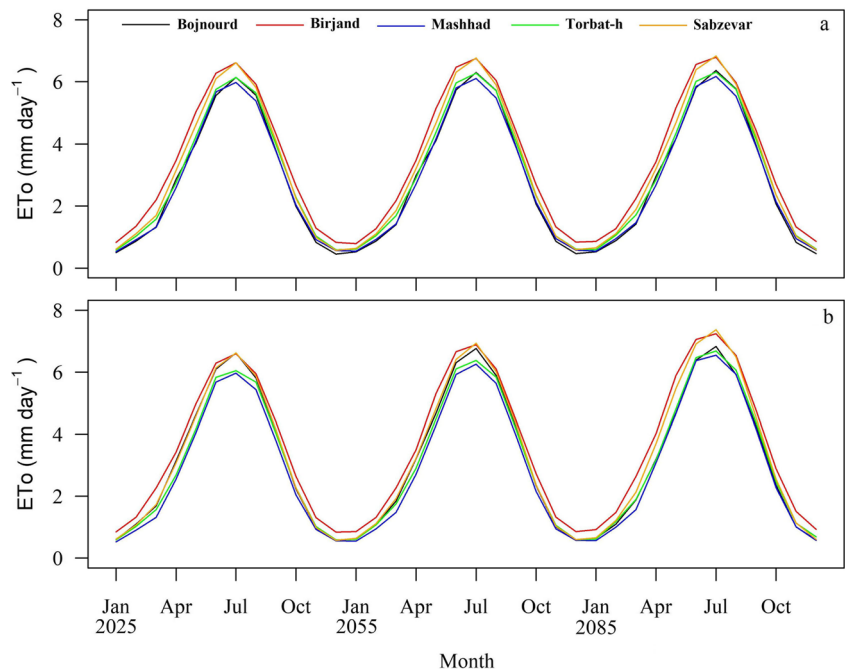
### 3.1 Evaluation of the climate model

The precise projection of climatic parameters such as precipitation and temperature for the baseline period shows the accuracy of downscaling methods in climate change assessments (Viglizzo et al. 1997). The results listed in Tables 3, 4, and 5 show that MarkSimGCM adequately well synthesized  $T_{\min}$ ,  $T_{\max}$ , and precipitation time series for the baseline period (1961–1990). Despite the

**Table 6** Baseline climate characteristics for monthly maximum temperature, minimum temperature, precipitation, and solar radiation (1961–1990)

Location	January	February	March	April	May	June	July	August	September	October	November	December
<b>Maximum temperature (°C)</b>												
Bojnourd	5.6	8.6	12.5	20.2	26.0	30.9	33.7	33.5	28.5	21.4	12.5	6.9
Birjand	11.8	14.1	19.1	24.4	30.5	35.0	36.1	35.2	32.1	26.9	18.8	13.6
Mashhad	7.0	8.3	12.9	19.9	25.9	31.1	32.6	32.2	28.0	21.6	15.5	9.2
Torbat-h	7.5	9.9	14.3	19.7	26.5	31.7	33.1	32.9	29.1	23.3	15.8	10.2
Sabzevar	8.9	11.9	16.2	22.8	28.9	34.2	36.7	36.2	31.5	24.8	16.4	10.4
<b>Minimum temperature (°C)</b>												
Bojnourd	-4.4	-3.0	1.1	6.2	12.1	15.5	18.2	16.9	12.1	6.3	0.2	-3.7
Birjand	-0.9	0.7	5.6	9.5	14.7	18.0	20.2	17.9	13.0	7.8	2.1	-1.3
Mashhad	-4.8	-2.3	1.2	6.8	12.7	15.5	16.9	15.1	10.8	5.5	0.9	-1.8
Torbat-h	-4.2	-2.0	1.9	6.5	11.4	15.4	17.9	16.4	11.3	5.9	0.5	-2.9
Sabzevar	-2.7	-0.7	3.8	8.2	14.1	18.1	20.7	18.2	13.8	8.3	2.4	-2.1
<b>Rainfall (mm)</b>												
Bojnourd	28.9	25.1	52.5	56.1	40.2	10.6	9.1	3.8	8.1	12.3	20.1	17.2
Birjand	35.2	19.6	24.8	14.7	17.3	4.9	0.1	1.4	2.4	4.9	22.8	20.0
Mashhad	33.6	38.5	65.3	43.1	44.5	7.8	5.2	0.4	5.7	17.1	20.7	22.6
Torbat-h	49.9	30.8	52.9	45.7	40.5	6.1	1.0	0.3	0.4	5.4	16.6	27.6
Sabzevar	37.2	22.5	40.2	32.8	41.9	6.4	5.8	0.1	1.5	11.4	16.8	23.3
<b>Radiation (MJ m<sup>-2</sup> day<sup>-1</sup>)</b>												
Bojnourd	5.4	6.6	9.0	14.8	19.7	24.2	25.8	24.7	20.4	15.1	9.7	6.3
Birjand	7.5	8.2	12.9	16.5	22.3	25.3	25.9	25.1	21.5	17.3	12.3	8.9
Mashhad	6.4	6.6	9.5	13.1	19.5	24.5	25.6	24.5	20.5	15.5	10.6	7.6
Torbat-h	6.3	7.5	10.8	13.8	20.8	24.5	25.1	24.7	20.8	16.2	11.2	8.1
Sabzevar	6.0	7.7	11.1	15.4	21.4	25.1	26.5	25.1	20.8	16.0	10.7	7.3

**Fig. 3** The future monthly ET<sub>0</sub> under both emission pathways (a RCP-4.5 and b RCP-8.5)



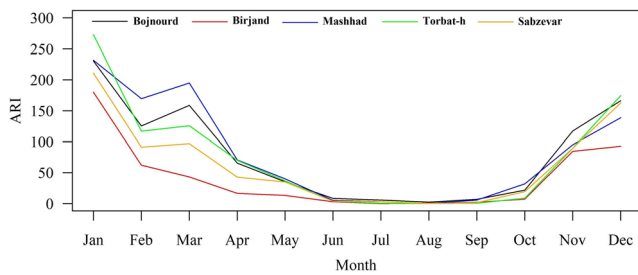


**Fig. 4** The monthly ARI series for the baseline period (1961–1990)

significant differences between modeled and observed  $T_{max}$  and precipitation in Mashhad and Sabzevar and also  $T_{min}$  in Sabzevar during summer (Tables 3, 4, and 5), MarkSimGCM performed acceptably well in generating  $T_{min}$ ,  $T_{max}$ , and precipitation over 1961–1990.

### 3.2 Reference evapotranspiration

The mean monthly  $ET_0$  series for the baseline period are shown in Fig. 2. The lowest mean monthly  $ET_0$  was often obtained in January, while the greatest mean monthly  $ET_0$  was found in July (Fig. 2). Over our study area, the lowest and highest  $T_{min}$  and  $T_{max}$  were mostly observed in January and July, respectively (Table 6). In addition, maximum and minimum solar radiation values were, respectively, in July and January (Table 6). In general, the highest mean monthly  $ET_0$  in July can be accounted for by the hot and dry summer in this month (Chowdhury et al. 2016). Wang et al. (2007) also stated that the changes in  $ET_0$  values were greater in winter and summer months compared with those in autumn and spring months. Moreover, Birjand (the most arid site) and Bojnourd (the wettest location) with 1200.31 and

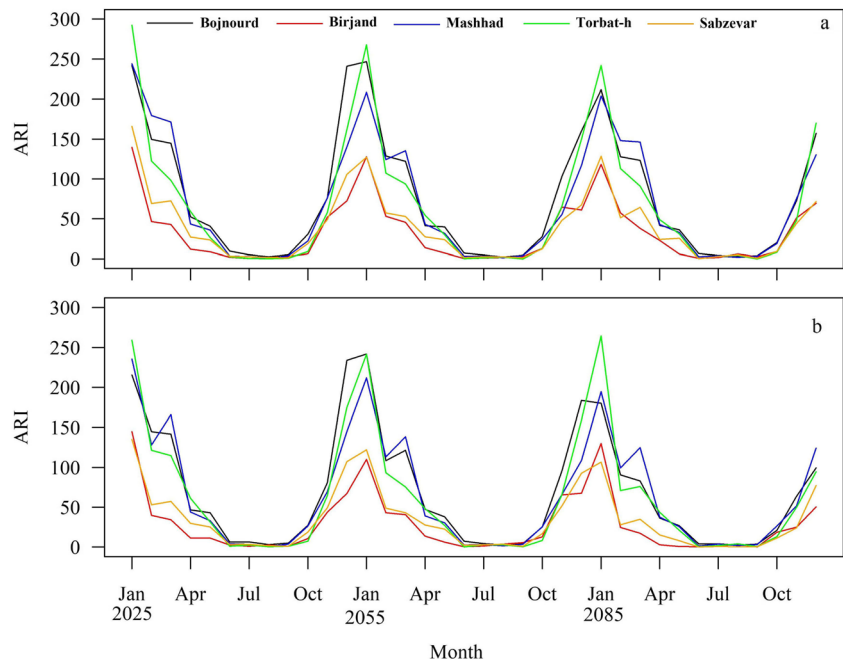
**Table 7** The modified Kc values for different growth phases of winter wheat

Location	Initial	Mid-season	Late season
Bojnourd	0.4	1.19	0.25
Birjand	0.4	1.21	0.25
Mashhad	0.4	1.16	0.25
Torbat-h	0.4	1.17	0.25
Sabzevar	0.4	1.21	0.25

991.05 mm also showed the highest and lowest mean annual  $ET_0$  values, respectively, among all sites in the baseline period.

The mean monthly  $ET_0$  values will increase in the 2025s, 2055s, and 2085s relative to the baseline period under RCP-4.5 and RCP-8.5 over the investigated stations (Fig. 3). The highest mean monthly  $ET_0$  rise was projected for the late twenty-first century (the 2085s). The average increases in mean monthly  $ET_0$  for RCP-4.5 and RCP-8.5 were 3.6 and 4% over the 2025s, 6.3 and 8.8% in the 2055s, and also 7 and 16.7% during the 2085s, respectively. In general, the mean monthly  $ET_0$  values in January will increase from 5.88 to 13.46% under RCP-4.5 and 10.71 to 20.93% under RCP-8.5 in the 2085s over our study area. The increment in July will also be from 5.93 to 6.88% and 12.95 to 15.33% under RCP-4.5 and RCP-8.5 in the 2085s at all study locations, respectively. Therefore, the projected change in mean monthly  $ET_0$  was more noticeable under RCP-8.5 vis-à-vis under RCP-4.5. Rodríguez Díaz et al. (2007) projected

**Fig. 5** The future monthly ARI under both emission pathways (a RCP-4.5 and b RCP-8.5)





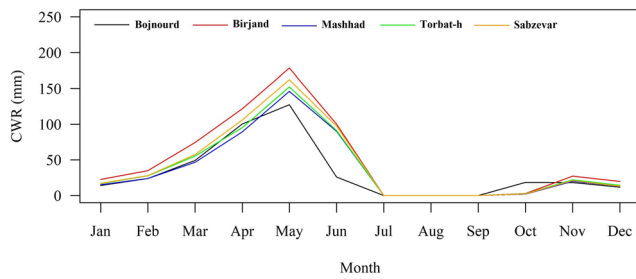


**Fig. 6** The monthly CWR series for the baseline period (1961–1990)

around 8% increase in  $ET_0$  over Spain in the mid-twenty-first century.

### 3.3 Agricultural rainfall index

The frequency and persistence of dry spells over the surveyed sites for 1961–1990 (baseline period) were determined using the mean monthly ARI (Fig. 4). Each month with the ARI value less than 40 was considered as dry. Accordingly, the frequency of dry months was calculated to be about 59.17, 79.72, 60, 66.11, and 61.67% for Bojnourd, Birjand, Mashhad, Sabzevar, and Torbat-h in 1961–1990, respectively. The highest mean monthly ARI value was found in January, while the lowest was often obtained in August which can be attributed to high  $ET_0$  and the lowest precipitation in August (Fig. 4). Moreover, the greatest and lowest mean monthly ARI values (272.94 and 0.05) were also obtained for Torbat-h and Birjand, respectively. The longest dry spell was observed from April to November in Birjand and from May to November at other areas in the baseline period (Fig. 4). A prolonged dry spell is likely to hamper crop development creating a need for

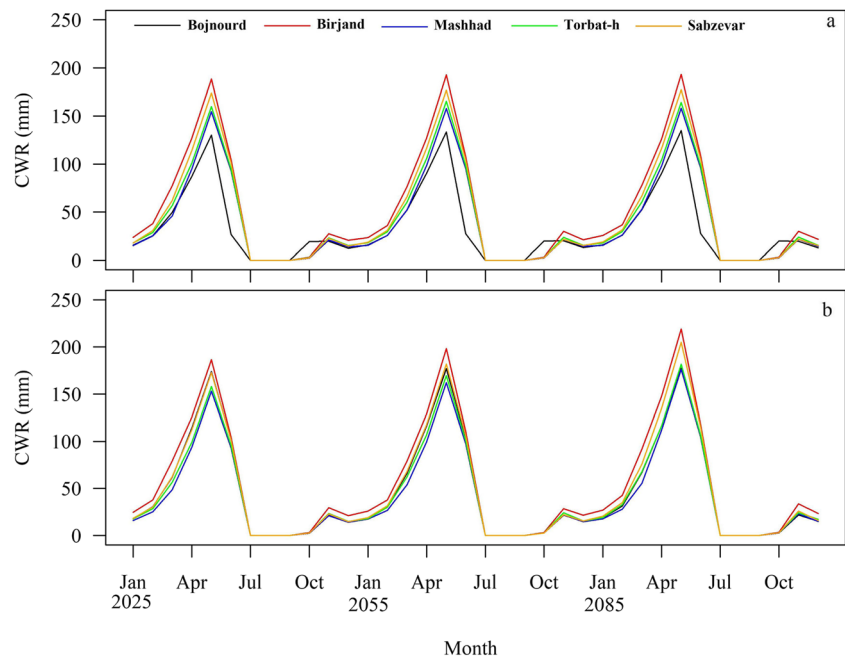
supplemental irrigation in dryland farming systems (Sayari et al. 2013; Nouri et al. 2017a, d).

Except for Bojnourd during the 2025s, the mean monthly ARI would likely decrease under all scenarios and time slices over the studied regions (Fig. 5). The mean monthly ARI reduction was greater for RCP-8.5 indicating more intense and long-lasting droughts under this pathway (Fig. 5). Across all sites, the mean monthly ARI values were projected to decline from  $-18.81$  to  $-82.59$  under RCP-4.5 and  $-31.62$  to  $-104.56$  under RCP-8.5 during the 2085s. Furthermore, the highest and lowest mean monthly ARI changes are, respectively, expected in Sabzevar ( $-18.81$ ) and Bojnourd ( $-104.56$ ) (Fig. 5). Sayari et al. (2013) also projected a higher drought frequency due to global warming in northeastern Iran.

### 3.4 Crop water requirement

The corrected  $Kc_{mid}$ , according to the regional climatic conditions, is shown in Table 7. The minimum mean monthly CWR was found in October for all areas as rainfed wheat is in its initial stage of growth in this month (Fig. 6). The mean monthly CWR was also lower in December with respect to that in November due to the lower solar radiation and crop evapotranspiration as well as higher precipitation in this month (Fig. 6). In general,  $Kc$  increment during the wheat growing period can lead to greater CWR. With regard to the results, wheat mostly showed the highest water requirement in May because of higher temperature and solar radiation and lower rainfall during this month (Fig. 6). It is noteworthy that the mean monthly CWR in June decreased as wheat is at the final phase of growth and the rate of crop physiological

**Fig. 7** The future monthly CWR under both emission pathways (a RCP-4.5 and b RCP-8.5)



processes such as respiration and photosynthesis is low in this month (Fig. 6). In general, among all studied regions, the highest and lowest mean monthly CWR in May were obtained in Birjand and Bojnourd, respectively. Moreover, on an annual scale, the highest and lowest average CWR were found in Birjand (567.32 mm) and Bojnourd (384.49 mm), respectively.

The mean monthly CWR is anticipated to increase over the twenty-first century relative to the baseline period in the studied sites (Fig. 7). The highest mean monthly CWR increment was projected in the 2085s for RCP-8.5. The mean monthly CWR increase would be due mainly to global air temperature warming. It should be noted that 1 °C increase of temperature is likely to enhance CWR by 2.9% in water-limited regions (Chowdhury et al. 2016). Enhanced CWR imposes a considerable stress on the non-renewable groundwater resources in arid regions (Chowdhury et al. 2016). The highest and lowest changes in mean monthly CWR were, respectively, modeled in Sabzevar (26.24%) under RCP-8.5 and in Bojnourd (5.91%) under RCP-4.5 in the 2085s. Chowdhury et al. (2016) also reported an increment in CWR ranging from 5.3 to 9.6% under CC in an arid region located in the Middle East over 2011–2050.

### 3.5 Projection of future changes in wheat yield, WUE, and PUE

The rainfed wheat yield, WUE, and PUE were projected to decrease under both emission scenarios and future time periods relative to the baseline for all studied areas (Fig. 8). The ranges of simulated wheat yield, WUE, and PUE among all sites were from 840 to 87 kg ha<sup>-1</sup>, 3.9 to 1 kg ha<sup>-1</sup> mm<sup>-1</sup>, and also 4.5 to 1.2 kg ha<sup>-1</sup> mm<sup>-1</sup> under RCP-4.5 and RCP-8.5 in the 2025s and 2085s in Bojnourd and Birjand, respectively. In general, grain yield, WUE, and PUE will be more negatively affected by CC under RCP-8.5. In addition, a greater decrease of PUE, WUE, and yield is highly likely during the late twenty-first century (Fig. 8). These results are in agreement with those reported by Kattge and Knorr (2007), Asseng et al. (2011), Xiao and Tao (2014), and Paymard et al. (2018). Among all sites, the highest reduction of yield (34.55–78.83%), WUE (30.76–61.54%), and PUE (34.01–76.19%) is anticipated in Birjand (the most arid station). Moreover, the lowest decline in yield (12.59–39.75%), WUE (9.30–30.23%), and PUE (10.25–35.89%) was simulated for Bojnourd (the wettest site) under the emission pathways (Fig. 8). The PUE values were lower than WUE values in the future. This is due to the fact that ET<sub>c</sub> is only one of the loss components of the hydrological cycle. According to Eqs. 3 and 4, a lower quantity of PUE is hence expected with respect to WUE (Wang et al. 2016). Overall, PUE seems to be better suited for elucidating the association between precipitation and final yield.

## 4 Conclusions

The results reveal that the least and greatest mean monthly ET<sub>0</sub> were, respectively, determined in January and July in the baseline period over the studied regions. A positive trend in mean monthly ET<sub>0</sub> is anticipated through the current century. A larger increase of mean monthly ET<sub>0</sub> was projected in the 2085s and under RCP-8.5. The longest dry spell was determined from April to November in Birjand and from May to November at other study locations in the baseline period. Furthermore, the mean monthly ARI will likely decrease under both emission pathways with respect to the baseline period over the studied locations. The minimum and maximum mean

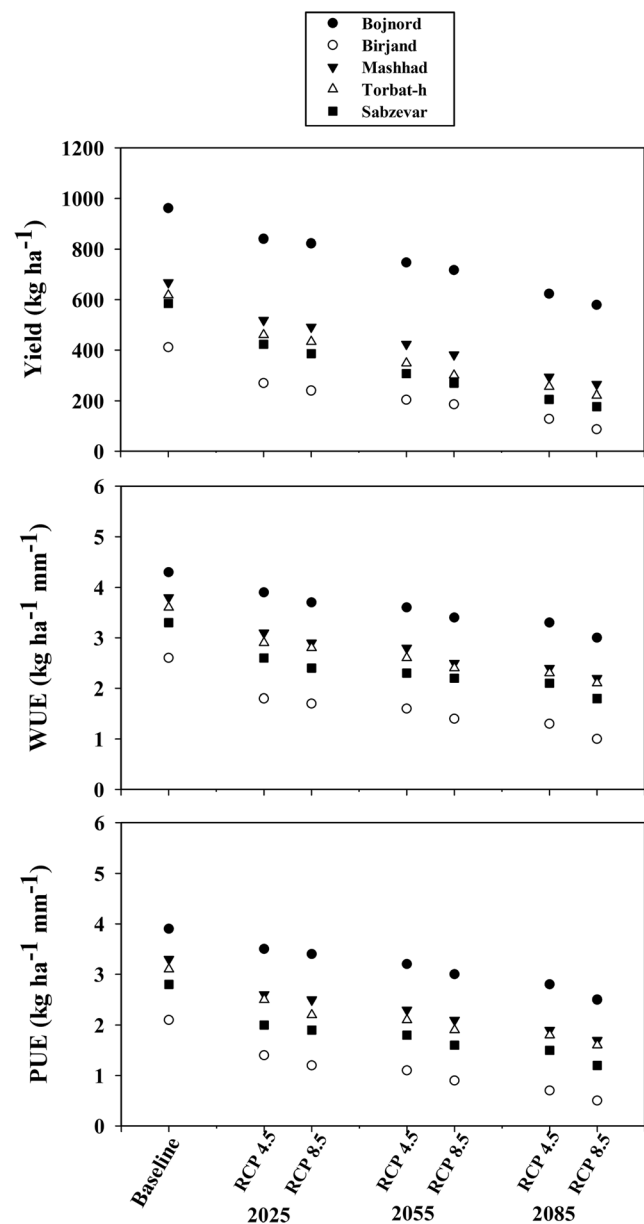


Fig. 8 Rainfed wheat yield, WUE, and PUE in the baseline period (1961–1990) and future

monthly CWR were found in October and May during the period of 1961–1990, respectively. Further, the mean monthly CWR will rise over the twenty-first century due to CC. The greatest mean monthly CWR increment was projected for the 2085s under RCP-8.5 scenario. Wheat grain yield, WUE, and PUE would likely decrease under both emission pathways over the investigated regions. The highest and smallest reductions in rainfed wheat yield, WUE, and PUE were, respectively, simulated for Birjand (the most arid site) and Bojnourd (the wettest location) in the future. Rainfed cereal production seems therefore to be adversely impacted by CC in northeastern Iran. Adopting appropriate adaptive strategies such as changing cropping patterns, applying fertilizer, increasing plant density, using appropriate cultivars, and sowing date appears to be of great importance to reduce climate change's negative effects and avoid national food insecurity.

## References

- Allen RG, Pereira LS, Raes D, Smith M (1998) Crop evapotranspiration: guidelines for computing crop water requirements. FAO irrigation and drainage paper No. 56. FAO, Rome
- Araghi A, Mousavi-Baygi M, Adamowski J (2015) Detection of trends in days with extreme temperatures in Iran from 1961 to 2010. *Theor Appl Climatol* 125:213–225. <https://doi.org/10.1007/s00704-015-1499-6>
- Araghi A, Martinez CJ, Adamowski J, Olesen JE (2018) Spatiotemporal variations of aridity in Iran using high-resolution gridded data. *Int J Climatol* 38:2701–2717. <https://doi.org/10.1002/joc.5454>
- Ashofteh P-S, Haddad OB, Mariño MA (2015) Risk analysis of water demand for agricultural crops under climate change. *J Hydrol Eng* 20(4):04014060. [https://doi.org/10.1061/\(ASCE\)HE.1943-5584.0001053](https://doi.org/10.1061/(ASCE)HE.1943-5584.0001053)
- Asseng S, Foster IAN, Turner NC (2011) The impact of temperature variability on wheat yields. *Glob Chang Biol* 17:997–1012. <https://doi.org/10.1111/j.1365-2486.2010.02262.x>
- Bannayan M, Eyshi Rezaei E (2014) Future production of rainfed wheat in Iran (Khorasan province): climate change scenario analysis. *Mitig Adapt Strateg Glob Chang* 19:211–227. <https://doi.org/10.1007/s11027-012-9435-x>
- Bannayan M, Sanjani S, Alizadeh A, Lotfabadi SS, Mohamadian A (2010) Association between climate indices, aridity index, and rainfed crop yield in northeast of Iran. *Field Crop Res* 118:105–114. <https://doi.org/10.1016/j.fcr.2010.04.011>
- Bannayan M, Lotfabadi SS, Sanjani S, Mohamadian A, Aghaalikhani M (2011) Effects of precipitation and temperature on crop production variability in northeast Iran. *Int J Biometeorol* 55:387–401. <https://doi.org/10.1007/s00484-010-0348-7>
- Bannayan M, Mansoori H, Rezaei EE (2014) Estimating climate change, CO<sub>2</sub> and technology development effects on wheat yield in northeast Iran. *Int J Biometeorol* 58:395–405. <https://doi.org/10.1007/s00484-013-0635-1>
- Bannayan M, Paymard P, Ashraf B (2016) Vulnerability of maize production under future climate change: possible adaptation strategies. *J Sci Food Agric* 96:4465–4474. <https://doi.org/10.1002/jsfa.7659>
- Cai W, Borlace S, Lengaigne M, Van Rensch P, Collins M, Vecchi G, Timmermann A, Santoso A, McPhaden MJ, Wu L (2014) Increasing frequency of extreme El Niño events due to greenhouse warming. *Nat Clim Chang* 4:111–116. <https://doi.org/10.1038/nclimate2100>
- Cai W, Santoso A, Wang G, Yeh SW, An SI, Cobb KM, Collins M, Guilyardi E, Jin FF, Kug JS, Lengaigne M, McPhaden MJ, Takahashi K, Timmermann A, Vecchi G, Watanabe M, Wu L (2015) ENSO and greenhouse warming. *Nat Clim Chang* 5:849–859. <https://doi.org/10.1038/nclimate2743>
- Chowdhury S, Al-Zahrani M, Abbas A (2016) Implications of climate change on crop water requirements in arid region: an example of Al-Jouf, Saudi Arabia. *J King Saud Univ Eng Sci* 28:21–31. <https://doi.org/10.1016/j.jksues.2013.11.001>
- Doorenbos J, Kassam A (1979) Yield response to water. FAO irrigation and drainage paper No. 33. FAO, Rome
- Dufresne JL, Foujols MA, Denvil S, Caubel A, Marti O, Aumont O, Balkanski Y, Bekki S, Bellenger H, Benshila R, Bony S, Bopp L, Braconnot P, Brockmann P, Cadule P, Cheruy F, Codron F, Cozic A, Cugnet D, de Noblet N, Duvel JP, Ethé C, Fairhead L, Fichefet T, Flavoni S, Friedlingstein P, Grandpeix JY, Guez L, Guilyardi E, Hauglustaine D, Hourdin F, Idelkadi A, Ghattas J, Joussaume S, Kageyama M, Krinner G, Labetoulle S, Lahellec A, Lefebvre MP, Lefevre F, Levy C, Li ZX, Lloyd J, Lott F, Madec G, Mancip M, Marchand M, Masson S, Meurdesoif Y, Mignot J, Musat I, Parouty S, Polcher J, Rio C, Schulz M, Swingedouw D, Szopa S, Talandier C, Terray P, Viovy N, Vuichard N (2013) Climate change projections using the IPSL-CM5 earth system model: from CMIP3 to CMIP5. *Clim Dyn* 40:2123–2165. <https://doi.org/10.1007/s00382-012-1636-1>
- Dunne JP, John JG, Adcroft AJ, Griffies SM, Hallberg RW, Shevliakova E, Stouffer RJ, Cooke W, Dunne KA, Harrison MJ, Krasting JP, Malyshev SL, Milly PCD, Philipps PJ, Sentman LT, Samuels BL, Spelman MJ, Winton M, Wittenberg AT, Zadeh N (2012) GFDL-ESM2 global coupled climate-carbon earth system models. Part I: physical formulation and baseline simulation characteristics. *J Clim* 25:6646–6665. <https://doi.org/10.1175/JCLI-D-11-00560.1>
- Evans JP (2009) Twenty-first century climate change in the Middle East. *Clim Chang* 92:417–432. <https://doi.org/10.1007/s10584-008-9438-5>
- Eyshi Rezaei E, Bannayan M (2012) Rainfed wheat yields under climate change in northeastern Iran. *Meteorol Appl* 19:346–354. <https://doi.org/10.1002/met.268>
- FAO (2009) CROPWAT 8.0 software: a computer program for irrigation planning and management. Land and water division of FAO; Available at: <http://www.fao.org/land-water/databases-and-software/cropwat/en>
- Faramarzi M, Yang H, Schulin R, Abbaspour KC (2010) Modeling wheat yield and crop water productivity in Iran: implications of agricultural water management for wheat production. *Agric Water Manag* 97:1861–1875. <https://doi.org/10.1016/j.agwat.2010.07.002>
- Ghazalli MZ, Nieuwolt S (1982) The use of an agricultural rainfall index in Malaysia. *Int J Biometeorol* 26:277–283. <https://doi.org/10.1007/bf02219494>
- Guo R, Lin Z, Mo X, Yang C (2010) Responses of crop yield and water use efficiency to climate change in the North China Plain. *Agric Water Manag* 97:1185–1194. <https://doi.org/10.1016/j.agwat.2009.07.006>
- Hoogenboom G, Porter CH, Shelia V, Boote KJ, Singh U, White JW, Hunt LA, Ogoshi R, Lizaso JI, Koo J, Asseng S, Singels A, Moreno LP, Jones JW (2017) Decision support system for agrotechnology transfer (DSSAT) version 4.7 (www.DSSAT.net). DSSAT Foundation, Gainesville, Florida, USA
- Huang J, Yu H, Dai A, Wei Y, Kang L (2017) Drylands face potential threat under 2 °C global warming target. *Nat Clim Chang* 7:417–422. <https://doi.org/10.1038/NCLIMATE3275>
- Hutchinson MF (1997) ANUSPLIN version 3.2 users guide. The Australian National University, Centre for Resource and Environmental Studies, Canberra

- IPCC (2013) Climate Change 2013: The physical science basis. contribution of working group I to the fifth assessment report of the Intergovernmental panel on Climate Change. Cambridge University Press, Cambridge, United Kingdom and New York, NY, USA. <https://doi.org/10.1017/CBO9781107415324>
- Jensen ME, Allen RG (2016) Evaporation, evapotranspiration, and irrigation water requirements. ASCE manuals and reports on engineering practice No. 70, 2nd edn. American Society of Civil Engineers, Reston. <https://doi.org/10.1061/9780784414057>
- Jones PG, Thornton PK (2013) Generating downscaled weather data from a suite of climate models for agricultural modelling applications. *Agric Syst* 114:1–5. <https://doi.org/10.1016/j.agry.2012.08.002>
- Jones PG, Thornton PK (2015) Representative soil profiles for the Harmonized World Soil Database at different spatial resolutions for agricultural modelling applications. *Agric Syst* 139:93–99. <https://doi.org/10.1016/j.agry.2015.07.003>
- Jones JW, Hoogenboom G, Porter CH, Boote KJ, Batchelor WD, Hunt LA, Wilkens PW, Singh U, Gijsman AJ, Ritchie JT (2003) The DSSAT cropping system model. *Eur J Agron* 18:235–265. [https://doi.org/10.1016/S1161-0301\(02\)00107-7](https://doi.org/10.1016/S1161-0301(02)00107-7)
- Kattge J, Knorr W (2007) Temperature acclimation in a biochemical model of photosynthesis: a reanalysis of data from 36 species. *Plant Cell Environ* 30:1176–1190. <https://doi.org/10.1111/j.1365-3040.2007.01690.x>
- Li Y, Ye W, Wang M, Yan X (2009) Climate change and drought: a risk assessment of crop-yield impacts. *Clim Res* 39:31–46. <https://doi.org/10.3354/cr00797>
- Luo X, Xia J, Yang H (2015) Modeling water requirements of major crops and their responses to climate change in the North China Plain. *Environ Earth Sci* 74:3531–3541. <https://doi.org/10.1007/s12665-015-4400-0>
- Iran Ministry of Agriculture (2015) Statistical analysis of crop yields and harvested areas during last 36 years (1979–2014). Office of Statistics and Information Technology, Ministry of Agriculture, Tehran, Iran
- Mo X, Liu S, Lin Z, Guo R (2009) Regional crop yield, water consumption and water use efficiency and their responses to climate change in the North China Plain. *Agric Ecosyst Environ* 134:67–78. <https://doi.org/10.1016/j.agee.2009.05.017>
- Nieuwolt S (1989) Estimating the agricultural risks of tropical rainfall. *Agric For Meteorol* 45:251–263. [https://doi.org/10.1016/0168-1923\(89\)90047-6](https://doi.org/10.1016/0168-1923(89)90047-6)
- Nouri M, Homae M (2018) On modeling reference crop evapotranspiration under lack of reliable data over Iran. *J Hydrol* 566:705–718. <https://doi.org/10.1016/j.jhydrol.2018.09.037>
- Nouri M, Homae M, Bannayan M, Hoogenboom G (2016) Towards modeling soil texture-specific sensitivity of wheat yield and water balance to climatic changes. *Agric Water Manage* 177:248–263. <https://doi.org/10.1016/j.agwat.2016.07.025>
- Nouri M, Homae M, Bannayan M (2017a) Climate variability impacts on rainfed cereal yields in west and northwest Iran. *Int J Biometeorol* 61:1571–1583. <https://doi.org/10.1007/s00484-017-1336-y>
- Nouri M, Homae M, Bannayan M (2017b) Quantitative trend, sensitivity and contribution analyses of reference evapotranspiration in some arid environments under climate change. *Water Resour Manag* 31:2207–2224. <https://doi.org/10.1007/s11269-017-1638-1>
- Nouri M, Homae M, Bannayan M (2017c) Spatiotemporal reference evapotranspiration changes in humid and semi-arid regions of Iran: past trends and future projections. *Theor Appl Climatol* 133:361–375. <https://doi.org/10.1007/s00704-017-2176-8>
- Nouri M, Homae M, Bannayan M, Hoogenboom G (2017d) Towards shifting planting date as an adaptation practice for rainfed wheat response to climate change. *Agric Water Manage* 186:108–119. <https://doi.org/10.1016/j.agwat.2017.03.004>
- Paymard P, Bannayan M, Sadrabadi Haghghi R (2018) Analysis of the climate change effect on wheat production systems and investigate the potential of management strategies. *Nat Hazards* 91:1237–1255. <https://doi.org/10.1007/s11069-018-3180-8>
- Penman HL (1948) Natural evaporation from open water, bare soil and grass. *Proc R Soc Lond A Math Phys Sci* 193:120–145. <https://doi.org/10.1098/rspa.1948.0037>
- Pereira AR (2004) The Priestley–Taylor parameter and the decoupling factor for estimating reference evapotranspiration. *Agric For Meteorol* 125:305–313. <https://doi.org/10.1016/j.agrformet.2004.04.002>
- Peterson GA, Westfall DG (2004) Managing precipitation use in sustainable dryland agroecosystems. *Ann Appl Biol* 144:127–138. <https://doi.org/10.1111/j.1744-7348.2004.tb00326.x>
- Priestley CHB, Taylor RJ (1972) On the assessment of surface heat flux and evaporation using large-scale parameters. *Mon Weather Rev* 100:81–92. [https://doi.org/10.1175/1520-0493\(1972\)100<0081:otaosh>2.3.co;2](https://doi.org/10.1175/1520-0493(1972)100<0081:otaosh>2.3.co;2)
- Riahi K, Rao S, Krey V, Cho C, Chirkov V, Fischer G, Kindermann G, Nakicenovic N, Rafaj P (2011) RCP 8.5—a scenario of comparatively high greenhouse gas emissions. *Clim Chang* 109:33–57. <https://doi.org/10.1007/s10584-011-0149-y>
- Richardson CW (1981) Stochastic simulation of daily precipitation, temperature, and solar radiation. *Water Resour Res* 17:182–190. <https://doi.org/10.1029/WR017i001p00182>
- Rockström J, Barron J, Fox P (2002) Rainwater management for increased productivity among small-holder farmers in drought prone environments. *Phys Chem Earth, Parts A/B/C* 27:949–959. [https://doi.org/10.1016/S1474-7065\(02\)00098-0](https://doi.org/10.1016/S1474-7065(02)00098-0)
- Rockström J, Falkenmark M, Karlberg L, Hoff H, Rost S, Gerten D (2009) Future water availability for global food production: the potential of green water for increasing resilience to global change. *Water Resour Res* 45:W00A12. <https://doi.org/10.1029/2007WR006767>
- Rockström J, Karlberg L, Wani SP, Barron J, Hatibu N, Oweis T, Bruggeman A, Farahani J, Qiang Z (2010) Managing water in rainfed agriculture—the need for a paradigm shift. *Agric Water Manag* 97:543–550. <https://doi.org/10.1016/j.agwat.2009.09.009>
- Rodríguez Diaz JA, Weatherhead EK, Knox JW, Camacho E (2007) Climate change impacts on irrigation water requirements in the Guadalquivir river basin in Spain. *Reg Environ Chang* 7:149–159. <https://doi.org/10.1007/s10113-007-0035-3>
- Sayari N, Bannayan M, Alizadeh A, Farid A (2013) Using drought indices to assess climate change impacts on drought conditions in the northeast of Iran (case study: Kashafood basin). *Meteorol Appl* 20:115–127. <https://doi.org/10.1002/met.1347>
- Song Z, Qiao F, Song Y (2012) Response of the equatorial basin-wide SST to wave mixing in a climate model: an amendment to tropical bias. *J Geophys Res* 117:C00J26. <https://doi.org/10.1029/2012JC007931>
- Sowers J, Vengosh A, Weinthal E (2011) Climate change, water resources, and the politics of adaptation in the Middle East and North Africa. *Clim Chang* 104:599–627. <https://doi.org/10.1007/s10584-010-9835-4>
- Stewart BA, Steiner JL (1990) Water-use efficiency. In: Singh RP, Parr JF, Stewart BA (eds) *Advances in soil science: dryland agriculture: strategies for sustainability*. Springer New York, New York, pp 151–173. [https://doi.org/10.1007/978-1-4613-8982-8\\_7](https://doi.org/10.1007/978-1-4613-8982-8_7)
- Tabari H, Marofi S, Aeiini A, Talaei PH, Mohammadi K (2011) Trend analysis of reference evapotranspiration in the western half of Iran. *Agric For Meteorol* 151:128–136. <https://doi.org/10.1016/j.agrformet.2010.09.009>
- Thomson AM, Calvin KV, Smith SJ, Kyle GP, Volke A, Patel P, Delgado-Arias S, Bond-Lamberty B, Wise MA, Clarke LE, Edmonds JA (2011) RCP4.5: a pathway for stabilization of radiative forcing by



2100. *Clim Chang* 109:77–94. <https://doi.org/10.1007/s10584-011-0151-4>
- Todorovic M (2005) Crop Evapotranspiration. In: Lehr LH, Keeley J (eds) *Surface and agricultural water*, Water Encyclopedia, vol 3. Wiley-Interscience, Hoboken, New Jersey, USA, pp 571–579. <https://doi.org/10.1002/047147844X.aw57>
- Viglizzo E, Roberto Z, Lértora F, Gay EL, Bernardos J (1997) Climate and land-use change in field-crop ecosystems of Argentina. *Agric Ecosyst Environ* 66:61–70. [https://doi.org/10.1016/S0167-8809\(97\)00079-0](https://doi.org/10.1016/S0167-8809(97)00079-0)
- Wang Y, Jiang T, Bothe O, Fraedrich K (2007) Changes of pan evaporation and reference evapotranspiration in the Yangtze River basin. *Theor Appl Climatol* 90:13–23. <https://doi.org/10.1007/s00704-006-0276-y>
- Wang J, Wang E, Liu DL (2011) Modelling the impacts of climate change on wheat yield and field water balance over the Murray–Darling basin in Australia. *Theor Appl Climatol* 104:285–300. <https://doi.org/10.1007/s00704-010-0343-2>
- Wang X, Cai D, Wu H, Hoogmoed W, Oenema O (2016) Effects of variation in rainfall on rainfed crop yields and water use in dryland farming areas in China. *Arid Land Res Manag* 30:1–24. <https://doi.org/10.1080/15324982.2015.1012686>
- Watanabe S, Hajima T, Sudo K, Nagashima T, Takemura T, Okajima H, Nozawa T, Kawase H, Abe M, Yokohata T, Ise T, Sato H, Kato E, Takata K, Emori S, Kawamiya M (2011) MIROC-ESM2010: model description and basic results of CMIP5-20c3m experiments. *Geosci Model Dev* 4:845–872. <https://doi.org/10.5194/gmd-4-845-2011>
- Wu T (2012) A mass-flux cumulus parameterization scheme for largescale models: description and test with observations. *Clim Dyn* 38:725–744. <https://doi.org/10.1007/s00382-011-0995-3>
- Xiao D, Tao F (2014) Contributions of cultivars, management and climate change to winter wheat yield in the North China Plain in the past three decades. *Eur J Agron* 52(Part B):112–122. <https://doi.org/10.1016/j.eja.2013.09.020>
- Yang X, Gao W, Shi Q, Chen F, Chu Q (2013) Impact of climate change on the water requirement of summer maize in the Huang-Huai-Hai farming region. *Agric Water Manag* 124:20–27. <https://doi.org/10.1016/j.agwat.2013.03.017>
- Yang Y, Liu DL, Anwar MR, O’Leary G, Macadam I, Yang Y (2016) Water use efficiency and crop water balance of rainfed wheat in a semi-arid environment: sensitivity of future changes to projected climate changes and soil type. *Theor Appl Climatol* 123:565–579. <https://doi.org/10.1007/s00704-015-1376-3>

**Publisher’s note** Springer Nature remains neutral with regard to jurisdictional claims in published maps and institutional affiliations.